J|A|C|S ARTICLES

Published on Web 07/06/2009

Response of Small-Scale, Methyl Rotors to Protein−Ligand Association: A Simulation Analysis of Calmodulin−Peptide Binding

Marimuthu Krishnan*,† and Jeremy C. Smith†,‡

UT/ORNL Center for Molecular Biophysics, Oak Ridge National Laboratory, Oak Ridge, Tennessee 37831, and Department of Biochemistry and Cellular and Molecular Biology, University of Tennessee, Knoxville, Tennessee 37996

Received February 18, 2009; E-mail: krishnanm@ornl.gov

Abstract: Changes in the free energy barrier (ΔE), entropy, and motional parameters associated with the rotation of methyl groups in a protein (calmodulin (CaM)) on binding a ligand (the calmodulin-binding domain of smooth-muscle myosin (smMLCKp)) are investigated using molecular dynamics simulation. In both the bound and uncomplexed forms of CaM, the methyl rotational free energy barriers follow skewed-Gaussian distributions that are not altered significantly upon ligand binding. However, site-specific perturbations are found. Around 11% of the methyl groups in CaM exhibit changes in ΔE greater than 0.7 kcal/mol on binding. The rotational entropies of the methyl groups exhibit a nonlinear dependence on ΔE. The relations are examined between motional parameters (the methyl rotational NMR order parameter and the relaxation time) and ΔE. Low-barrier methyl group rotational order parameters deviate from ideal tetrahedrality by up to ∼20%. There is a correlation between rotational barrier changes and proximity to the protein-peptide binding interface. Methyl groups that exhibit large changes in ΔE are found to report on elements in the protein undergoing structural change on binding.

1. Introduction

A molecular-level understanding of how ligands recognize and bind to proteins is of fundamental importance in biology and medicine. Upon ligand binding, the protein potential energy surface is perturbed, and consequently, changes occur in the protein structure, dynamics (both vibrational and conformational) and associated thermodynamics.[1] For example, associating molecules reorganize structurally while losing significant amounts of rotational and translational entropy.[2−4] Further, the conformational entropy of a protein can be significantly changed upon ligand binding.[5−13]

Since thermodynamic properties, such as the entropy and heat capacity, depend on the internal dynamics of proteins, it is essential to characterize dynamical changes on binding, and these have been the focus of many recent biophysical studies.[5−15] Of particular interest among the experimental techniques used is nuclear magnetic resonance (NMR) spectroscopy. ^{15}N NMR relaxation data provide information on amide backbone fluctuations, while ^{13}C, ^{1}H and ^{2}H relaxation spectra of methyl-bearing residues have been used to examine side-chain motions.[5−13]

The Lipari-Szabo "model-free" formalism is often used to interpret NMR spectral data in terms of fluctuations of bond vectors (amide N−H vectors for backbone dynamics and C−H vectors of methyl groups for side-chain dynamics), yielding an order parameter, O^2, quantifying the amplitude of motion and a corresponding relaxation time, τ.[16,17] By expressing O^2 and the conformational entropy in terms of the orientational probability distribution functions of the bond vector, a connection between dynamics measured by NMR and the thermodynamics of proteins can be established.[14,15,18−21] In this way, recent high-resolution, site-specific NMR experiments have furnished microscopic details pertaining to ligand-induced changes in the

† Oak Ridge National Laboratory.
‡ University of Tennessee.

(1) Balog, E.; Becker, T.; Oettl, M.; Lechner, R.; Daniel, R.; Finney, J.; Smith, J. C. *Phys. Rev. Lett.* **2004**, *93*, 28103.
(2) Steinberg, I. Z.; Scheraga, H. A. *J. Biol. Chem.* **1963**, *238*, 172–181.
(3) Schwarzl, S. M.; Tschopp, T. B.; Smith, J. C.; Fischer, S. *J. Comput. Chem.* **2002**, *23*, 1143–1149.
(4) Grater, F.; Schwarzl, S. M.; Dejaegere, A.; Fischer, S.; Smith, J. C. *J. Phys. Chem. B* **2005**, *109*, 10474–10483.
(5) Lee, A. L.; Kinnear, S. A.; Wand, A. J. *Nat. Struct. Biol.* **2000**, *7*, 72–77.
(6) Frederick, K. K.; Marlow, M. S.; Valentine, K. G.; Wand, A. J. *Nature* **2007**, *448*, 325–329.
(7) Prabhu, N. V.; Lee, A. L.; Wand, A. J.; Sharp, K. A. *Biochemistry* **2003**, *42*, 562–570.
(8) Wand, A. J. *Nat. Struct. Biol.* **2001**, *8*, 926–31.
(9) Lee, A. L.; Wand, A. J. *Nature* **2001**, *411*, 501–504.
(10) Igumenova, T. I.; Frederick, K. K.; Wand, A. J. *Chem. Rev.* **2006**, *106*, 1672–99.
(11) Lee, A. L.; Flynn, P. F.; Wand, A. J. *J. Am. Chem. Soc.* **1999**, *121*, 2891–2902.
(12) Ishima, R.; Torchia, D. A. *Nat. Struct. Biol.* **2000**, *7*, 740–743.
(13) Ishima, R.; Petkova, P.; Louis, J. M.; Torchia, D. A. *J. Am. Chem. Soc.* **2001**, *123*, 6164–6171.
(14) Yang, D.; Kay, L. E. *J. Mol. Biol.* **1996**, *263*, 369–382.
(15) Li, Z.; Raychaudhuri, S.; Wand, A. J. *Protein Sci.* **1996**, *5*, 2647–2650.
(16) Lipari, G.; Szabo, A. *J. Am. Chem. Soc.* **1982**, *104*, 4546–4559.
(17) Lipari, G.; Szabo, A. *J. Am. Chem. Soc.* **1982**, *104*, 4559–4570.
(18) Zdek, L.; Novotny, M. V.; Stone, M. J. *Nat. Struct. Biol.* **1999**, *6*, 1118–1121.
(19) Akke, M.; Brueschweiler, R.; Palmer, A. G., III *J. Am. Chem. Soc.* **1993**, *115*, 9832–9833.
(20) Johnson, E.; Chazin, W. J.; Rance, M. *J. Mol. Biol.* **2006**, *357*, 1237–1252.
(21) LeMaster, D. M. *J. Am. Chem. Soc.* **1999**, *121*, 1726–1742.

dynamics and thermodynamics of calcium-saturated calmodulin (CaM) upon complexation with the calmodulin-binding domain of smooth-muscle myosin (smMLCKp).[5−11] It was found that CaM exhibits significant changes in side-chain dynamics while the backbone dynamics is apparently unaffected by the binding process.

Methyl rotational relaxations in proteins can be described as rotation of C−H vectors about the symmetry axis, characterized by a corresponding NMR order parameter O^2_{rot}, superposed on the reorientational dynamics of the symmetry axis itself, with associated order parameter O^2_{axis}. The experimentally determined order parameter, O^2, is then the product:

$$O^2 = O^2_{\mathrm{rot}} O^2_{\mathrm{axis}} \tag{1}$$

In most experimental NMR analyses, it has been assumed that all methyl groups in a protein possess ideal tetrahedral geometry and exhibit hindered rotation about their symmetry axes leading to $O^2_{\mathrm{rot}} = 0.111$.[22] Given this assumption experiments provide O^2_{axis}, obtained as $O^2/0.111$.

NMR, neutron scattering experiments and molecular dynamics (MD) simulations have shown that the rotational barriers of methyl groups in proteins and peptide crystals can be strongly affected by packing effects relative to the gas phase.[23−28] Unlike hydrocarbon crystals, in which methyl groups often experience almost identical environments, in a protein each methyl group experiences a different environment, giving rise to packing-sensitive, heterogeneous methyl rotational dynamics.[23,24,29,30] A systematic understanding of how environmental factors (such as, for example, the degree of solvent exposure, variations in van der Waals and electrostatic interactions, and local packing density) affect the rotational barriers (ΔE) is still lacking. Also of interest is a recent study investigating the low-temperature physics of a protein crystal, which has shown that methyl groups located near the internal cavities (regions with less packing) of a protein may exhibit barrier reduction relative to the gas phase and with increasing temperature may also trigger low-temperature anharmonic dynamics[30] incipient at the dynamical "glass" transition of proteins.[31−33]

Both NMR and neutron scattering experiments can used to determine ΔE. In neutron scattering the distribution of rotational barriers in a polymer, $g(\Delta E)$, has been estimated from analysis of the variation with temperature of the elastically scattered intensity.[34,35] Subsequently, if $g(\Delta E)$ is approximated as a Gaussian the methyl group relaxation spectrum can be derived.[31,34] Similarly, neutron scattering experiments on lysozyme in solution have been interpreted using a Gaussian distribution of methyl rotational barrier heights centered at 3.98 kcal/mol with a width of 1.39 kcal/mol.[31]

In NMR experiments, ^{1}H and ^{2}H spin relaxation times are used to determine ΔE. In ^{1}H relaxation studies, by fitting the Arrhenius equation to the temperature dependence of the ^{1}H NMR spin−lattice relaxation time (T_1), methyl rotational barriers can be obtained for proteins in the solid state.[36] In ^{2}H relaxation studies, fitting the temperature-dependence of the Lipari-Szabo τ with the Arrhenius equation determines ΔE for each methyl site.[26] A recent NMR study has suggested ΔE to be an useful parameter for assessing the quality of NMR-derived structures.[26]

In this report we characterize the changes in the site-specific rotational dynamics and thermodynamics of methyl groups in CaM upon binding of smMLCKp using all-atom molecular dynamics (MD) simulations. To accurately determine the free energy barrier, ΔE, the umbrella sampling method is used. Both for the bound and unbound forms of CaM the dynamic and thermodynamic properties of the individual methyl groups are averaged over an ensemble of 6 independent MD trajectories. The dependence of the dynamical and thermodynamic properties (obtained from the MD simulations) on ΔE (obtained from umbrella sampling) is examined.

The results are used to address a number of questions concerning how the rotational dynamics of methyl groups is affected by ligand binding. The relation is examined between the NMR motional parameters (τ and O^2_{rot}) and ΔE, and how τ and O^2_{rot} vary upon ligand binding. We also determine the dependence on ΔE of the methyl rotational entropy.

The results indicate that a significant fraction of methyl groups in CaM exhibit large changes in ΔE upon ligand binding. Some of these are buried at the protein−ligand binding interface and are found to report on structural changes in "latch" region of the protein. The results suggest that site-specific methyl groups might potentially be useful as experimental probes in molecular recognition.

2. Simulation Details

Molecular dynamics simulations of Ca^{2+}-saturated CaM (PDB id: 1CLL) and the CaM/smMLCKp complex (PDB id: 1CDL) were carried out using NAMD[37] with the CHARMM27 all-atom[38] and TIP3P water[39] force fields. The initial configuration of the CaM/smMLCKp complex was taken from the 2.4 Å resolution crystal structure (PDB id: 1CDL) which contains four replicas in the asymmetric unit of the crystal.[40] Of these, Replica B was chosen as it contains only two missing atoms, apart from five residues that are missing in all replicas. The missing residues were built and hydrogens added using CHARMM. The initial structure of Ca^{2+}-saturated CaM was taken from the crystal structure refined at 1.7 Å using X-ray crystallography (PDB id: 1CLL).[41]

(22) Chatfield, D. C.; Szabo, A.; Brooks, B. R. *J. Am. Chem. Soc.* **1998**, *120*, 5301–5311.
(23) Baudry, J.; Smith, J. C. *J. Phys. Chem. B* **2005**, *109*, 20572–20578.
(24) Kitson, D. H.; Hagler, A. T. *Biochemistry* **1988**, *27*, 5246–5257.
(25) Chatfield, D. C.; Wong, S. E. *J. Phys. Chem. B* **2000**, *104*, 11342–11348.
(26) Xue, Y.; Pavlova, M. S.; Ryabov, Y. E.; Reif, B.; Skrynnikov, N. R. *J. Am. Chem. Soc.* **2007**, *129*, 6827–6838.
(27) Batchelder, L. S.; Niu, C. H.; Torchia, D. A. *J. Am. Chem. Soc.* **1983**, *105*, 2228–2231.
(28) Hu, H.; Hermans, J.; Lee, A. L. *J. Biomol. NMR* **2005**, *32*, 151–162.
(29) Baudry, J. *J. Am. Chem. Soc.* **2006**, *128*, 11088–11093.
(30) Krishnan, M.; Kurkal-Siebert, V.; Smith, J. C. *J. Phys. Chem. B* **2008**, *112*, 5522.
(31) Roh, J. H.; Novikov, V. N.; Gregory, R. B.; Curtis, J. E.; Chowdhuri, Z.; Sokolov, A. P. *Phys. Rev. Lett.* **2005**, *95*, 38101.
(32) Roh, J. H; Curtis, J. E; Azzam, S; Novikov, V. N; Peral, I; Chowdhuri, Z.; Gregory, R. B.; Sokolov, A. P. *Biophys. J.* **2006**, *91*, 2573.
(33) Hayward, J. A; Smith, J. C *Biophys. J.* **2002**, *82*, 1216–1225.
(34) Frick, B.; Fetters, L. J. *Macromolecules* **1994**, *27*, 974–980.
(35) Colmenero, J.; Moreno, A. J.; Alegra, A. *Prog. Polym. Sci.* **2005**, *30*, 1147–1184.
(36) Andrew, E. R.; Bryant, D. J.; Cashell, E. M. *Chem. Phys. Lett.* **1980**, *69*, 551–554.
(37) Phillips, J. C.; Braun, R.; Wang, W.; Gumbart, J.; Tajkhorshid, E.; Villa, E.; Chipot, C.; Skeel, R. D.; Kale, L.; Schulten, K. *J. Comput. Chem.* **2005**, *26*, 1781–1802.
(38) Mackerell, A. D.; et al. *J. Phys. Chem. B* **1998**, *102*, 3586–3616.
(39) Jorgensen, W. L.; Chandrasekhar, J.; Madura, J. D.; Impey, R. W.; Klein, M. L. *J. Chem. Phys.* **1983**, *79*, 926–935.
(40) Meador, W. E.; Means, A. R.; Quiocho, F. A. *Science* **1992**, *257*, 1251–1255.
(41) Chattopadhyaya, R.; Meador, W. E.; Means, A. R.; Quiocho, F. A. *J. Mol. Biol.* **1992**, *228*, 1177–1192.

The model systems were constructed by placing the CaM/peptide complex and Ca^{2+}-saturated CaM in solvent (TIP3P water) boxes of dimensions (60 × 54 × 54) Å^3 and (59 × 76 × 56) Å^3, respectively. The water molecules that were in hard contact with the protein (protein-water distance <2.5 Å) were removed. Both the CaM/peptide complex and the uncomplexed CaM were energy minimized to a root-mean-square (rms) energy gradient of 10^{-3} kcal/mol/Å.

The MD simulations were performed in the NPT ensemble at 300 K and 1 atm pressure using a Langevin thermostat and barostat with a damping coefficient of 5 ps^{-1}. The nonbonded pair-interaction potential was truncated at 12 Å and smoothed between 10 Å and 12 Å using a cubic switching function. Periodic boundary conditions were applied. Electrostatic interactions were computed using the Particle Mesh Ewald (PME) method with a real space cutoff of 13 Å and the reciprocal space interactions were computed on 64 × 60 × 60 (CaM + peptide) and 60 × 81 × 60 (CaM) grids using sixth-degree B-splines. The equations of motion were integrated with a time step of 1 fs. The systems were energy minimized and then heated to 300 K followed by 2 ns equilibration and 10 ns of production run. Five further, independent 10 ns production runs were also performed, starting from the final configuration obtained from the first 10 ns production run and with different initial velocities.

In the umbrella sampling calculations, harmonic constraining potentials (force constant = 100 kcal/mol/rad^2) were applied to methyl dihedral angles. For each methyl group, the dihedral angle was partitioned into windows of 4° spacing and within each window 450 ps productive umbrella dynamics were performed.[42] The Weighted Histogram Analysis Method (WHAM) was used to extract free energy profiles from the probability distributions.[43]

The rotational entropy (S_{rot}) of a methyl group can be derived from the probability density, $\rho(\theta)$, using the following relation:

$$S_{rot} = -k_B \int \rho(\theta) \ln \rho(\theta) d\theta \quad (2)$$

where k_B is the Boltzmann constant and θ is the angle of rotation of a methyl group. Here, the probability density, $\rho(\theta)$, was calculated by dividing θ into N bins of size $d\theta$ and distributing the values of θ calculated from MD trajectories into these bins. Following the method proposed in refs.[44] and,[45] the optimal bin size was determined by minimizing the following cost function with respect to $d\theta$,

$$C(d\theta) = \frac{2\langle K\rangle - \langle \Delta K^2\rangle}{d\theta^2} \quad (3)$$

where $\langle K\rangle$ and $\langle \Delta K^2\rangle$ are the mean and variance of the number of hits per bin, defined as follows:

$$\langle K\rangle = \frac{1}{N}\sum_{i=1}^{N} K_i \quad (4)$$

$$\langle \Delta K^2\rangle = \frac{1}{N}\sum_{i=1}^{N} (K_i - \langle K\rangle)^2 \quad (5)$$

where K_i is the number of hits in the ith bin. The optimal value of $d\theta$ was thus found to be 2°.

The total side chain conformational entropy was calculated from the angular probability density function, $\rho(\phi,\chi)$, where ϕ and χ are the polar and azimuthal angles defining the orientation of the terminal $C-CH_3$ bond vector. The time-dependent variation in ϕ is due to the fluctuations of the symmetry axis of the methyl group while variation in χ is due to rotameric transitions of the preceding dihedral. For each methyl-bearing residue, $\rho(\phi,\chi)$ was calculated from the MD trajectories by tracking the time evolution of ϕ and χ. The conformational entropy was calculated from $\rho(\phi,\chi)$ using the following equation,

$$S_{conf} = -k_B \iint \rho(\phi,\chi) \ln \rho(\phi,\chi) \sin(\phi) d\phi d\chi \quad (6)$$

3. Results and Discussion

Figure 1a and b show the MD-derived distribution of rotational free energy barriers of methyl groups in the bound and unbound forms of CaM. The barrier heights follow a skewed-Gaussian distribution in both forms. The barrier distribution is not altered significantly upon ligand binding.

In both the unbound and bound states of CaM, ~55% of the methyl groups have barriers between 3 and 4 kcal/mol (peaked at ~3.4 kcal/mol). Previously determined activation energies

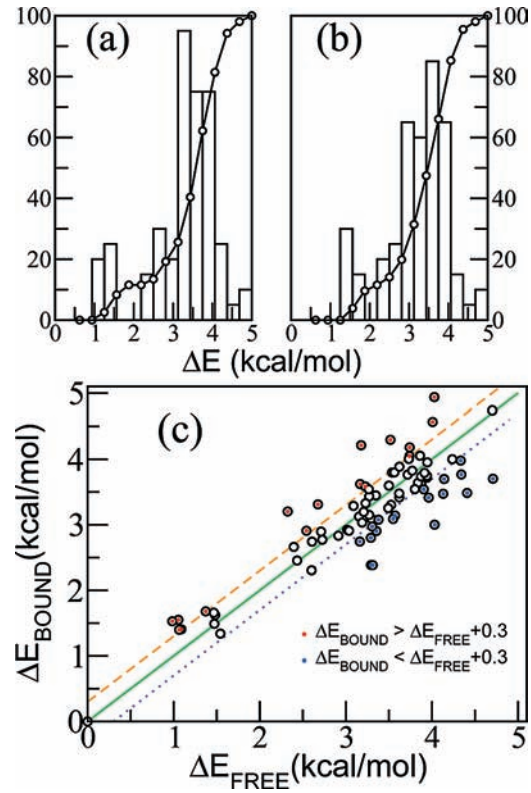

Figure 1. Distributions of rotational free energy barriers of methyl groups in (a) unbound and (b) bound states of CaM. The fraction of methyl groups (given as a percentage) with barrier heights less than a given value is also shown (solid line with a circle symbol). (c) Rotational free energy barriers of methyl groups in the bound (ΔE_{BOUND}) and unbound (ΔE_{FREE}) states are compared. The straight lines (solid, $\Delta E_{BOUND} = \Delta E_{FREE}$; dashed, $\Delta E_{BOUND} = \Delta E_{FREE} + 0.3$ kcal/mol; dotted, $\Delta E_{BOUND} = \Delta E_{FREE} - 0.3$ kcal/mol) are shown as guides to eyes.

(42) Torrie, G. M.; Valleau, J. P. *J. Comp. Phys.* **1977**, *23*, 187–199.
(43) Kumar, S.; Rosenberg, J. M.; Bouzida, D.; Swendsen, R. H.; Kollman, P. A. *J. Comput. Chem.* **1992**, *13*, 1011–1021.
(44) Shimazaki, H.; Shinomoto, S. *Adv. Neural Inf. Process. Syst.* **2007**, *19*, 1289.
(45) Shimazaki, H.; Shinomoto, S. *Neural Comput.* **2007**, *19*, 1503–1527.

Table 1. Ligand-Induced Changes in Methyl Rotational Barrier[a]

$\sum_{i=1}^{80}\Delta E_i$(bound) = 253.90 kcal/mol
$\sum_{i=1}^{80}\Delta E_i$(free) = 256.23 kcal/mol
$\sum_{i=1}^{80}(\Delta E_i(\text{bound}) - \Delta E_i(\text{free})) = -2.33$ kcal/mol
$\sum_{i=1}^{80}|\Delta E_i(\text{bound}) - \Delta E_i(\text{free})| = 26.40$ kcal/mol

[a] Here, ΔE_i denotes the rotational barrier of the ith methyl group.

Table 2. Methyl Groups in CaM that Exhibit Relatively Large Changes in $\Delta\Delta E$ Due to Ligand Binding Are Listed[a]

residue	$\Delta\Delta E$ (kcal/mol)	residue	$\Delta\Delta E$ (kcal/mol)
Val35$^{\gamma 1}$	1.03	Leu112$^{\delta 2}$	−1.04
Ala73	1.01	Thr146$^{\gamma 2}$	−0.91
Val142$^{\gamma 2}$	0.93	Val142$^{\gamma 1}$	−0.88
Ile125$^{\gamma 2}$	0.92	Leu4$^{\delta 2}$	−0.78
Leu18$^{\delta 1}$	0.91	Val35$^{\gamma 2}$	−0.64
Leu116$^{\delta 2}$	0.66		

[a] Here, $\Delta\Delta E = \Delta E$(free) − ΔE(bound).

associated with methyl rotation in both proteins and small molecules vary between ∼2 to ∼4 kcal/mol (excluding Met residues).[26,46,47] Those methyl groups with barriers <2 kcal/mol (11% of the methyl groups in CaM) are located in Met residues, and a slight net increase in these barriers is found upon ligand binding. Similarly, around 23% of the methyl groups have barriers below 3 kcal/mol in the unbound state while this figure is ∼27% in the unbound state. The similarity of the distributions in Figure 1a and b indicates that the barrier distribution alone does not furnish information on ligand-induced changes in protein dynamics.

A site-specific investigation of barrier changes provides insight into the dynamical perturbation. The per-site ΔE of methyl groups in the bound (ΔE_{BOUND}) and unbound (ΔE_{FREE}) states is shown in Figure 1c. The diagonal ($\Delta E_{\text{FREE}} = \Delta E_{\text{BOUND}}$) is the unperturbed case. A significant number of data points are located away from the diagonal, indicating that ligand binding significantly alters the rotational free energy surfaces of these methyl groups: ∼11% of methyl groups exhibit $a >$ 0.7 kcal/mol change in rotational barrier due to ligand binding. Data on the changes in rotational barriers are listed in Tables 1 and 2.

The rotational entropy, S_{rot}, was derived from the probability distribution, $\rho(\theta)$, using eq 2. Figure 2 shows the ΔE dependence of S_{rot} of methyl groups in the ligand-free and ligand-bound forms of CaM. In both forms, the rotational entropy of the methyl groups varies between ∼1.5 and ∼3 cal/mol/K. The methyl groups in Met residues have larger rotational entropies (∼3 cal/mol/K) while Ile125$^{\gamma 2}$, Val136$^{\gamma 2}$, Ala128 (unbound) and Ile125$^{\gamma 2}$, Val136$^{\gamma 2}$, Thr62, Thr70, Ala128, Ala10 (bound) have rotational entropies below ∼1.7 cal/mol/K.

To compare the magnitude of S_{rot} with the conformational entropy, S_{conf} was calculated using eq 6. S_{conf} of side chains of CaM varies between 2.5 and 6.7 cal/mol/K (with an average of 4 cal/mol/K) and between 2.4 and 6.9 cal/mol/K (with an average of 4.2 cal/mol/K) in the bound and unbound states, respectively. These numbers are consistent with experimental values reported for proteins, calculated from NMR experiments. For example, from NMR on human ubiquitin, each methyl-bearing residue, on average, was estimated to contribute about 5 cal/mol/K to the conformational entropy.[15] The above

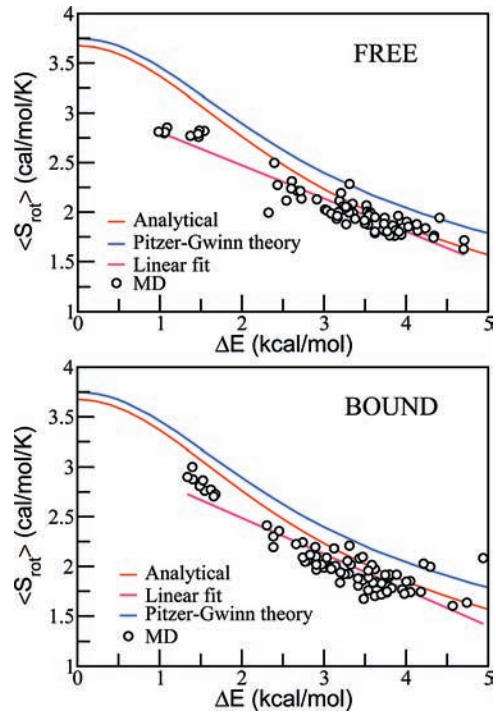

Figure 2. Rotational entropy (S_{rot}) versus rotational barrier (ΔE) of methyl groups in the bound and unbound states of CaM.

rotational entropies are significantly lower than the value of S_{rot} = 18.8 cal/mol/K for ethane in the gas phase at room temperature.[48]

It is evident from Figure 2 that S_{rot} calculated from MD trajectories increases with decrease in ΔE both in the bound and unbound forms of CaM. Both sets of data were fitted with a straight line, leading to the following relations

$$S_{\text{rot}}(\pm 0.11)(\text{cal/mol/K}) = 3.14(\pm 0.05) - 0.33(\pm 0.01)\Delta E(\text{free}) \quad (7)$$

$$S_{\text{rot}}(\pm 0.15)(\text{cal/mol/K}) = 3.21(\pm 0.07) - 0.36(\pm 0.02)\Delta E(\text{bound}) \quad (8)$$

We now further examine the relationship between ΔE and the rotational entropy. The potential of mean force (PMF), $F(\theta)$, profile associated with methyl rotation can be represented by a 3-fold symmetric function of the following form

$$F(\theta) = \frac{\Delta E}{2}[1 - \cos(3\theta - \theta_0)] \quad (9)$$

where θ_0 is the initial phase. The probability density function, $P(\theta)$, can be written as

$$P(\theta) = \frac{e^{-\beta F(\theta)}}{\int_0^{2\pi} e^{-\beta F(\theta)} d\theta} \quad (10)$$

Using eqs 2, 9 and 10, the relationship between S_{rot} and ΔE is obtained as follows

(46) Ramachandran, G. N.; Sasisekharan, V. *Adv. Protein Chem.* **1968**, *23*, 283–438.
(47) Keniry, M. A.; Kintanar, A.; Smith, R. L.; Gutowsky, H. S.; Oldfield, E. *Biochemistry* **1984**, *23*, 288–298.
(48) Tafipolsky, M.; Schmid, R. *J. Comput. Chem.* **2005**, *26*, 1579.

$$S_{rot} = \frac{-k_B \int_0^{2\pi} e^{-\beta F(\theta)}[-\beta F(\theta) - \ln(\int_0^{2\pi} e^{-\beta F(\theta)} d\theta)]d\theta}{\int_0^{2\pi} e^{-\beta F(\theta)} d\theta} \tag{11}$$

$$= \frac{k_B \beta \Delta E}{2} + k_B \ln\left[2\pi e^{-\beta \Delta E/2} I_0\left(\frac{\beta \Delta E}{2}\right)\right] - \frac{k_B \beta \Delta E}{2} \frac{I_1\left(\frac{\beta \Delta E}{2}\right)}{I_0\left(\frac{\beta \Delta E}{2}\right)} \tag{12}$$

where $I_n(x)$ is the n^{th}-order modified Bessel function of the first kind and it is defined as[49]

$$I_n(x) = \sum_{m=0}^{\infty} \frac{(-1)^m}{\Gamma(m+1)\Gamma(m+n+1)} \left(\frac{x}{2}\right)^{2m+n} \tag{13}$$

where Γ is the gamma function.[49]

The analytical solution relating S_{rot} and ΔE (expressed in eq 12) is also shown in Figure 2. Figure 2 shows that the values of S_{rot} calculated from MD simulations span the same range as that predicted by the analytical solution. In addition, the trend seen in the functional dependence of S_{rot} on ΔE obtained from MD simulations is similar to that predicted by eq 12 and is also consistent with the Pitzer-Gwinn statistical mechanical theory of methyl rotors developed in ref 50, in which the partition function for methyl rotors attached to a rigid molecular frame was derived using a simple model potential and then used to derive the thermodynamic functions. Note that the dependence of S_{rot} on ΔE predicted by Pitzer-Gwinn theory is sensitive to the value of the reciprocal of the partition function ($1/Q_f$) for free rotation as shown in Figure 3, where S_{rot} ($\Delta E = 0$) is plotted against ($1/Q_f$). The results obtained from the Pitzer-Gwinn model shown in Figure 2 correspond to $1/Q_f = 0.25$ while the analytical solution obtained in the present work corresponds to $1/Q_f = 0.261$. This provides the rationale for the differences between the analytical solution and Pitzer-Gwinn results shown in Figure 2.

The rotational entropic changes in the free energy induced by ligand binding are listed in Table 3. The total rotational entropic free energy of the complex is only 0.22 kcal/mol less than that of the unbound state. This result indicates that the entropic contribution associated with methyl rotation to the binding free energy is negligible.

To understand changes in methyl rotational dynamics upon ligand binding, we examine the relaxation behavior of the methyl C−H bond vectors ($\vec{r}_{\text{CH}}$) by calculating the rotational time correlation function, $C_{\text{NMR}}(t) = \langle P_2[\vec{r}_{\text{CH}}(0)\cdot\vec{r}_{\text{CH}}(t)]\rangle$, where $P_2[x]$ is the second-order Legendre polynomial. The subscript NMR indicates that this correlation function can, in principle, also be used to interpret NMR relaxation experiments. The brackets $\langle\rangle$ indicate an ensemble average over all three C−H vectors of a given methyl group and over all time origins in the simulation.

$C_{\text{NMR}}(t)$ was calculated as follows. For each methyl group, two consecutive rotations were performed such that the normal to the plane formed by the atoms C1, C2, and C3 (C1 denotes the methyl carbon and C1−C2 and C2−C3 are bonds medial to the methyl group) orients along the x-axis, and the bond vector connecting atom C1 and C2 is along the z-axis. The reorientational time correlation functions of the methyl C−H bond vectors were calculated in this frame of reference.

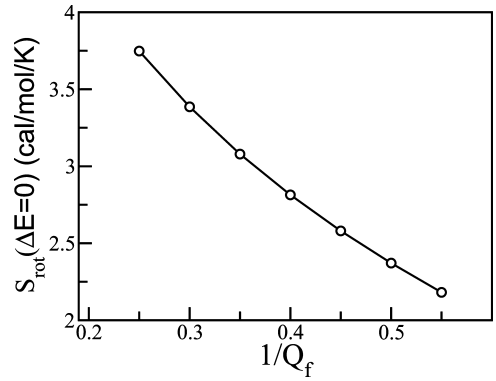

Figure 3. Rotational entropy of a barrier-free methyl rotor (S_{rot} ($\Delta E = 0$)) is shown as a function of the inverse partition function (obtained from Pitzer-Gwinn theory).

Table 3. Ligand-Induced Changes In Methyl Rotational Entropic Contributions to Free Energy[a]

$T\sum_{i=1}^{80} S^i_{\text{rot}}(\text{bound}) = 49.07$ kcal/mol
$T\sum_{i=1}^{80} S^i_{\text{rot}}(\text{free}) = 49.29$ kcal/mol
$T\sum_{i=1}^{80} (S^i_{\text{rot}}(\text{bound}) - S^i_{\text{rot}}(\text{free})) = -0.22$ kcal/mol
$T\sum_{i=1}^{80} \lvert S^i_{\text{rot}}(\text{bound}) - S^i_{\text{rot}}(\text{free})\rvert = 1.94$ kcal/mol

[a] Here, T is the temperature and S^i_{rot} denotes the rotational entropy of the i^{th} methyl group.

The computed rotational time correlation functions were fitted by a single exponential function of the form $C_{\text{NMR}}(t) = O^2_{\text{rot}} + (1 - O^2_{\text{rot}})e^{-t/\tau}$. Here, O^2_{rot} denotes the order parameter for the methyl group rotational dynamics and τ is the relaxation time associated with the methyl rotation.

The dependences of the motional parameters O^2_{rot} and τ on ΔE are now investigated. As mentioned in the Introduction, in the analysis of NMR experiments, it is generally assumed that all methyl groups in a protein have ideal tetrahedral geometry and that they exhibit hindered-rotation about their symmetry axes. The value of O^2_{rot} is 0.11 for a methyl group that rotates and possesses ideal tetrahedral geometry.[22] However, neutron diffraction studies of crystals of small peptides and NMR and molecular dynamics simulation of proteins have shown that some methyl groups deviate from tetrahedral geometry and indicate that O^2_{rot} can be lower (by ∼20%) than the ideal value of 0.11.[22,51−53]

Figure 4a shows O^2_{rot} as a function of ΔE. It is evident that $\langle O^2_{\text{rot}}\rangle$ increases with ΔE both in the bound and unbound states. Values of O^2_{rot} for methyl groups with lower barriers (<2.5 kcal/mol) are ∼20% smaller than the ideal value of 0.11, while for methyl groups having higher barriers the value of $\langle O^2_{\text{rot}}\rangle$ approaches the ideal value. To examine this geometrical variation more closely the deviation from ideal tetrahedrality was quantified by calculating the tetrahedral order parameter defined as follows:[54]

$$Q = 1 - \frac{3}{32} \sum_{i=1}^{3} \sum_{j=i+1}^{4} \left(\cos\phi + \frac{1}{3}\right)^2 \tag{14}$$

where ϕ is the angle subtended at the methyl carbon between the ith and jth bonds defining the tetrahedral group (the three C−H bonds and the C−CH_3 bond). Methyl groups with $Q = 1$ possess ideal tetrahedral geometry while those with $0 \le Q < 1$ deviate from the ideal case. Figure 4(b) demonstrates that Q

(49) Boas, M. *Mathematical methods in physical sciences*; Wiley: New York, 1983.
(50) Pitzer, K. S.; Gwinn, W. D. *J. Chem. Phys.* **1942**, *10*, 428–440.

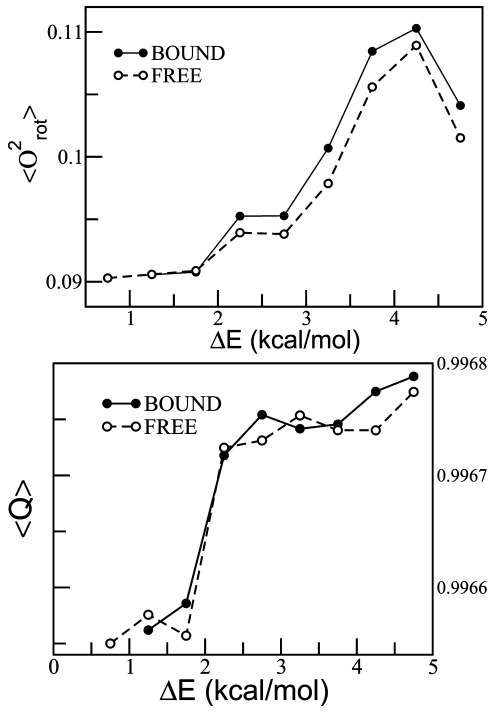

Figure 4. (a) $\langle O^2_{rot} \rangle$ and (b) $\langle Q \rangle$ as a function of ΔE. Here, $\langle O^2_{rot} \rangle$ and $\langle Q \rangle$ denote the average values of O^2_{rot} and Q averaged over windows of size $\Delta E = 0.5$ kcal/mol.

increases with ΔE, indicating that the methyl groups with large rotational barriers are more closely tetrahedral than those with lower ΔE.

Nine dihedral degrees of freedom contribute to the torsional free energy profile of a methyl group. At room temperature the contribution to the methyl barrier per degree of freedom is much less than the thermal energy and thus all methyl groups in a protein exhibit rotational dynamics, leading to values of $\langle O^2_{rot} \rangle$ close to the ideal value. At low temperatures, at which the contribution per degree of freedom to a methyl barrier is almost equal to, or slightly greater than, the thermal energy (the "landscape-dominated" regime), the values of $\langle O^2_{rot} \rangle$ vary between 0.11 (for methyl groups in microenvironments facilitating the rotational dynamics) and 1 (for strongly hindered rotors). The wide variation in O^2_{rot} at low temperatures suggests that the commonly used assumption that $O^2 = O^2_{rot}O^2_{axis} = 0.11O^2_{axis}$ may not be valid for those methyl groups in strong steric environments. A recent study investigating the low-temperature dynamics of crystalline myoglobin has shown a systematic nonlinear dependence of $\langle O^2_{rot} \rangle$ on ΔE.[30]

Figure 5 shows the methyl group rotational relaxation times, τ, as a function of ΔE for both the bound and unbound states. The rotational relaxation times are widely distributed, indicating dynamical heterogeneity. In both the bound and uncomplexed forms of CaM ~93% of methyl groups have $\tau < 300$ ps, values comparable to those derived from recent NMR experiments and MD simulations on proteins.[26,32] A 5% decrease in the number

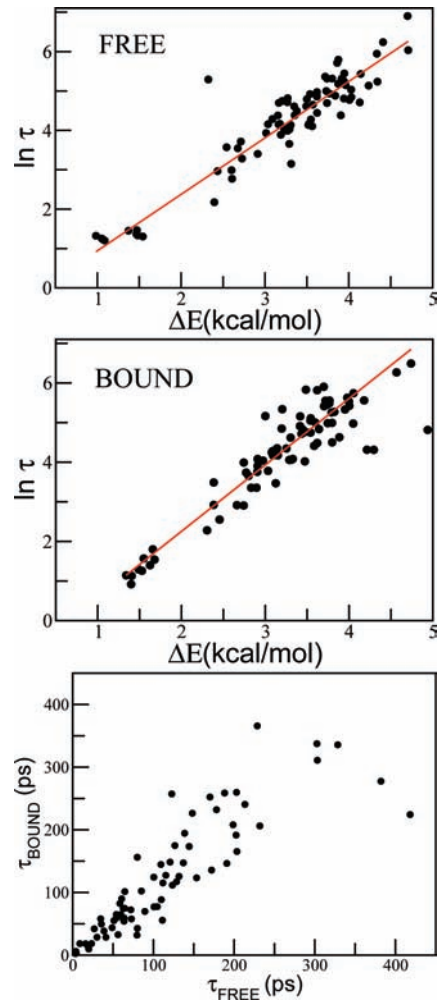

Figure 5. Rotational relaxation time (ln τ) versus rotational barrier (ΔE) of methyl groups in the (upper) unbound and (middle) bound states of CaM. (bottom) Rotational relaxation times of methyl groups in the bound (τ_{BOUND}) and unbound (τ_{FREE}) are compared.

of fast-relaxing methyl groups ($\tau \leq 150$ ps) is seen upon ligand binding (71% in the bound state and 76% in the unbound state).

In both the bound and unbound states a linear dependence of on ΔE is observed, suggesting that the generalized transition state theory can describe the activated rotational dynamics of methyl groups in proteins. Both sets of data were fitted with a straight line, leading to the following relations

$$\ln \tau(\pm 0.57) = -1.1(\pm 0.27) + 1.68(\pm 0.08)\Delta E(\text{bound}) \quad (15)$$

$$\ln \tau(\pm 0.47) = -0.49(\pm 0.21) + 1.43(\pm 0.06)\Delta E(\text{free}) \quad (16)$$

The generalized transition state theory (GTST) relates ln τ and ΔE using the following equation

$$\ln \tau = \ln\left(\frac{h}{\gamma k_B T}\right) + \frac{\Delta E}{k_B T} \quad (17)$$

where γ is the generalized transmission coefficient ($\gamma = 1$ for the nongeneralized transition state theory) and h is Planck's constant.[55] The transmission coefficients, calculated for the bound and unbound states by comparing eqs 15 and 16 with eq 17, are γ (bound) $= 0.48 \pm 0.13$ and γ (unbound) $= 0.26 \pm 0.05$. At 300 K, the value of k_BT is ~0.6 kcal/mol. The slope

(51) Lehmann, M. S.; Koetzle, T. F.; Hamilton, W. C. *J. Am. Chem. Soc.* **1972**, *94*, 2657–2660.
(52) Koetzle, T. F.; Golic, L.; Lehmann, M. S.; Verbist, J. J.; Hamilton, W. C. *J. Chem. Phys.* **1974**, *60*, 4690–4696.
(53) Ottiger, M.; Bax, A. *J. Am. Chem. Soc.* **1999**, *121*, 4690–4695.
(54) Chau, P. L.; Hardwick, A. J. *Mol. Phys.* **1998**, *93*, 511–518.
(55) Garcia-Viloca, M.; Gao, J.; Karplus, M.; Truhlar, D. G. *Science* **2004**, *303*, 186–195.

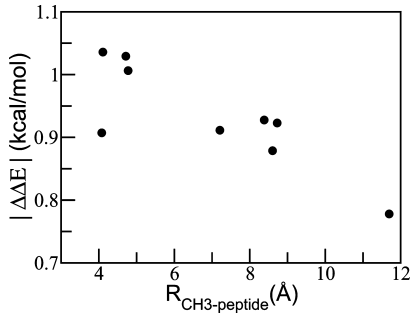

Figure 6. $\Delta\Delta E$ is shown as a function of the minimum distance between a methyl group and the peptide.

expected from GTST should be equal to $1/k_BT$, which is equal to 1.67 (kcal/mol)$^{-1}$ at 300 K. The slopes determined from our MD simulations are: 1.68 ± 0.08 (bound state) and 1.43 ± 0.06 (free state). Although the slope determined for the bound state is consistent with GTST, the deviation observed for the unbound state indicates the need for longer MD trajectories to better sample the conformational space of the protein to improve the accuracy of ΔE and τ. The comparison of τ for methyl groups in the bound (τ_{BOUND}) and unbound (τ_{FREE}) states indicates that the rotational relaxation behavior of certain site-specific methyl groups is significantly altered upon ligand binding.

The correlation between the changes in the rotational free energy barriers and proximity to the binding interface is now examined. In Figure 6, the absolute value of the ligand-induced change in the methyl rotational barrier, $\Delta\Delta E = |\Delta E_{bound} - \Delta E_{free}|$, is plotted as a function of $R_{CH_3-peptide}$, the minimum distance between the methyl carbon and peptide heavy atoms. The results are shown only for those 11% of the methyl groups in CaM that exhibit relatively large changes in $\Delta\Delta E$ (that is $\Delta\Delta E > 0.7$ kcal/mol, i.e., significantly higher than k_BT). These methyl groups are found on: Leu18$^{\delta 1}$, Val35$^{\gamma 1}$, Ala73$^{\beta}$, Leu112$^{\delta 2}$, Ile125$^{\gamma 2}$, Val142$^{\gamma 1}$, Val142$^{\gamma 2}$, and Thr146$^{\gamma 2}$. Among these, Leu18$^{\delta 1}$, Val35$^{\gamma 1}$, Ala73$^{\beta}$, Leu112$^{\delta 2}$ are proximal, being located close to the protein-peptide binding interface with $R_{CH_3-peptide} < 5.0$ Å, while the remaining methyl groups are distal with $R_{CH_3-peptide} > 7$ Å. It is evident from Figure 6 that there is a correlation between the rotational barrier change and proximity to the binding interface.

To examine the correlation between changes in the packing densities of the methyl groups and $\Delta\Delta E$, the solvent accessible surface area (A), at each configuration, was calculated (with a probe radius of 1.4 Å) for atoms within a distance (r_{cut}) from the methyl group. The local packing density, σ, was calculated using the following equation

$$\sigma = \left\langle \frac{N}{A r_{cut}} \right\rangle \tag{18}$$

where N is the number of neighboring atoms that are within a distance (r_{cut}) from the methyl group and the symbol $\langle\rangle$ denotes an average over different configurations sampled during MD simulations. The ligand-induced changes in the packing density of methyl groups were quantified by calculating $\Delta\sigma = |\sigma_{BOUND} - \sigma_{FREE}|$. Figure 7(a) shows $\Delta\sigma$ as a function of $R_{CH_3-peptide}$. While large changes in the packing density are observed for many methyl groups that are in close contact with the peptide, non-negligible changes in the packing density are also observed at distances further from the peptide ($R_{CH_3-peptide} \approx 8$ Å) indicating that ligand-induced perturbations are observed at

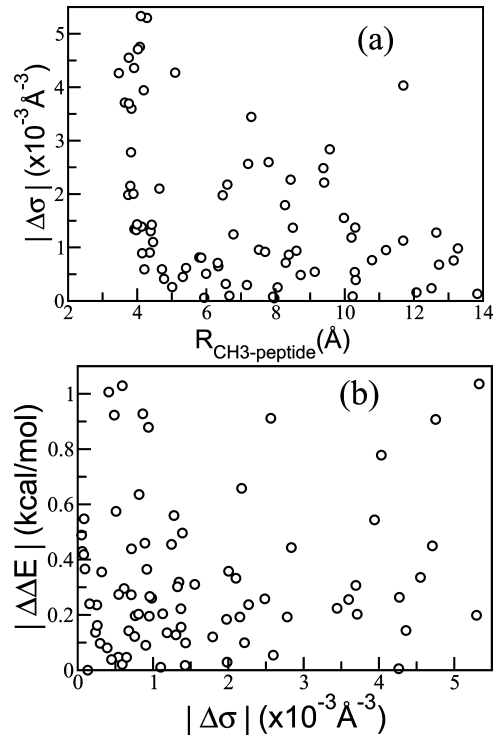

Figure 7. (a) $\Delta\sigma$ is shown as a function of the minimum distance between a methyl group and the peptide and (b) $\Delta\Delta E$ is shown as a function of $\Delta\sigma$.

distant structural sites far from the binding interface. Figure 7(b) shows $\Delta\sigma$ as a function of $\Delta\Delta E$. It is evident that the changes in the local packing density around methyl groups do not correlate with $\Delta\Delta E$.

We now examine more closely the location of those methyl groups that exhibit large ligand-induced changes in ΔE. It has been shown that methyl group rotational barriers are sensitive to variations in local van der Waals interactions.[25,29] The crystal structure of the CaM/smMLCKp complex shows that CaM engulfs the helical peptide, with the hydrophobic regions of CaM making many close van der Waals contacts with the hydrophobic side of the peptide.[40] Figure 8 shows the methyl groups with $\Delta\Delta E > 0.7$ kcal/mol together with the CaM-peptide complex.

Ala73$^{\beta}$ is part of Helix D (residues 65−74) that links the C-lobe to the N-lobe. The ligand binding is accompanied by unwinding of the central helix which also bends between residues 73 and 77. The large change in $\Delta\Delta E$ of Ala73$^{\beta}$ observed in the simulation can be attributed to this ligand-induced helix unwinding and bending.

A structure-based mechanism of the recognition of smMLCK by CaM suggests that the strong hydrophobic interaction between Helix B of the N-lobe and Helix F of the C-lobe serves as a latch to anchor the peptide.[40] Mutational studies have provided evidence in support of this mechanism and shown that smMLCK-activating residues are located in Helices B and F.[56] The proximal methyl groups (Leu18$^{\delta 1}$, Val35$^{\gamma 1}$, Leu112$^{\delta 2}$) that exhibit larger barrier changes ($\Delta\Delta E \geq 0.7$ kcal/mol) are located in the "latch" region,[40] where Helices B (residues 28−39), F (residues 101−112) and A (residues 5−20) of CaM are in close contact with each other.

The minimum distances between pairs of proximal methyl-bearing residues calculated from the MD trajectories in the

(56) Su, Z.; Fan, D.; George, S. E. *J. Biol. Chem.* **1994**, *269*, 16761–16765.

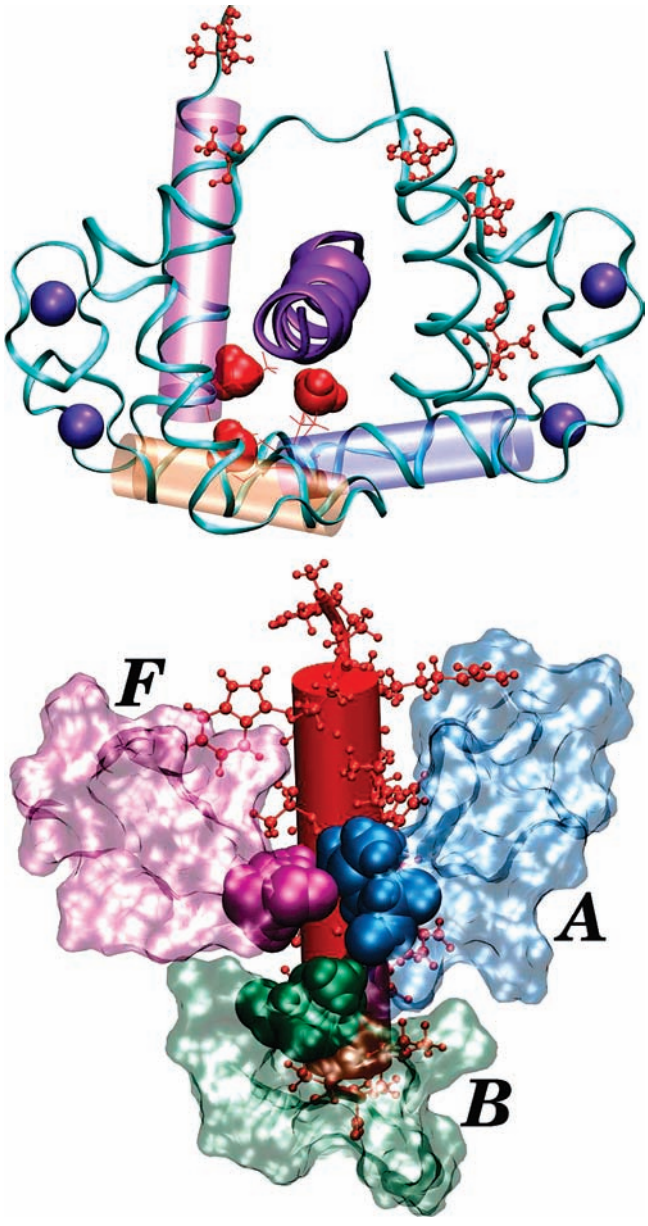

Figure 8. (top) Ball and stick representation of the methyl groups with $\Delta\Delta E$ greater than 0.7 kcal/mol are shown (red). CaM-peptide complex is shown in ribbon representation (CaM (green) the helical peptide (violet)). The violet van der Waals spheres denote the Ca^{2+} ions while the methyl groups that are in close proximity to the peptide are shown as van der Waals spheres (red). Helices A, B and F of CaM are shown as cylinders. (bottom) The "latch" region formed by Helices A, B, and F of CaM is shown together with the peptide (red). The proximal methyl groups that exhibit large barrier change are also shown as van der Waals spheres: Leu112 (magenta), Val35 (green), Leu18 (blue).

bound state are 3.95 Å, 3.83 Å, and 3.77 Å for Leu18-Val35, Leu18-Leu112 and Val35-Leu112, respectively, while these distances are 3.71 Å, 36.57 Å and 39.39 Å, respectively, in the unbound state. Therefore, an order of magnitude decrease in the minimum distances between Leu18 and Leu112 and between Val35 and Leu112 is observed upon ligand binding. This originates from the latch bringing Helices B and F in close proximity to each other.[40] The methyl groups in Leu18$^{\delta 1}$, Val35$^{\gamma 1}$, and Leu112$^{\delta 2}$ respond to these ligand-induced perturbations with large changes in their ΔE. Therefore, the present investigation, based on the dynamics of the free protein and the protein−ligand complex, suggests that methyl rotors located on these interacting helices recognize and respond strongly to ligand binding.

4. Conclusions

Ligand binding modifies the potential energy surface of a protein and, consequently, causes changes in the internal dynamics. The present work has investigated responses of methyl rotors in a test system involving binding of the calmodulin-binding domain of smooth-muscle myosin binding to CaM, using all-atom molecular dynamics simulations and umbrella sampling free energy calculation. The methyl rotors exhibit packing-sensitive, heterogeneous rotational dynamics and may therefore be of potential use as noninvasive probes in molecular recognition and ligand binding. To examine how rotational properties are affected by ligand binding, dynamic and thermodynamic properties of the methyl groups were calculated as averages over 6 independent 10 ns MD trajectories for both the bound and unbound forms.

In both the unbound and bound states of CaM, the calculated barrier heights follow a skewed-Gaussian distribution with ~55% of methyl groups possessing barriers between 3 and 4 kcal/mol and with a peak in the distributions around 3.4 kcal/mol. The barrier distribution is not altered significantly upon ligand binding. However, the differences between rotational barriers of individual methyl groups in the bound and unbound states indicate that ligand binding does significantly alter the rotational free energy surfaces of site-specific methyl rotors. Around 11% of the methyl groups in CaM exhibit greater than a 0.7 kcal/mol ΔE change.

The calculated rotational entropies, relaxation times and the rotational NMR order parameters of the methyl rotors in CaM are found to be correlated with the rotational barriers.

Methyl groups that exhibit relatively large changes in barrier are located close to the protein-peptide interface. The proximal methyl groups that exhibit large changes in ΔE are located in a region where Helices B (residues from 28 to 39), F (residues from 101 to 112) and A (residues from 5 to 20) of CaM come into close contact with each other on binding.

The findings in the present paper suggest that the experimental investigation of site-specific methyl rotational dynamics may provide useful information on local environmental changes on ligand binding. This site-specific information is in principle accessible to dynamic neutron scattering experiments, as rotational dynamical modifications will lead to modifications in quasielastic scattering. In practice, such experiments will require the preparation of specifically hydrogenated side-chains in an otherwise perdeuterated sample and significant incident neutron flux. Specific labeling of methyl groups in a protein for neutron scattering studies has been performed and the corresponding hydrogen probability density maps derived using the LADI diffractometer at the Institut Laue-Langevin, Grenoble (ILL).[57] Furthermore, experimental dynamic neutron scattering combined with isotope labeling has demonstrated that incoherent scattering from individual residue types is measurable with good counting statistics on the IN16 backscattering spectrometer at the ILL, and qualitative, interpretable differences were seen in the scattering between Ile, Tyr and Leu residues.[58] The

(57) Weiss, K. L.; Meilleur, F.; Blakeley, M. P.; Myles, D. A. A. *Acta Crystallogr., Sect. F: Struct. Biol. Cryst. Commun.* **2008**, *64*, 537–540.
(58) Wood, K.; Grudinin, S.; Kessler, B.; Weik, M.; Johnson, M.; Kneller, G. R.; Oesterhelt, D.; Zaccai, G. *J. Mol. Biol.* **2008**, *380*, 581–591.

combination of the above two advances with the significant improvement in counting statistics, relative to ILL, achievable on the new neutron sources such as the Spallation Neutron Source at Oak Ridge National Laboratory, indicates that the use of neutron scattering to characterize site-specific methyl group probability densities and dynamics is now practicable.

The above high-resolution neutron experiments, the existing theoretical tools for characterizing the neutron-scattering from methyl dynamics,[30,59] and the atomistic details obtained from our present MD simulations suggest a line of neutron scattering experimentation, involving specific hydrogenation of methyl-containing residues of protein−ligand complexes and proteases (for example, 50% of residues in HIV-protease contain methyl groups). In particular, the high-quality proton probability density maps and scattering functions obtained from these neutron experiments can be used to derive the experimental counterpart of the dynamic and thermodynamic quantities reported in our manuscript.

Similarly, NMR can be expected to provide information directly comparable with the present work. For example, ^{2}H NMR relaxation data of specifically labeled methyl sites in a 62-residue SH3 domain from chicken R-spectrin measured at different temperatures have determined the rotational barriers for 35 distinct methyl sites.[26] The ligand induced changes in barrier heights at different methyl sites can therefore in principle be measured using ^{2}H NMR relaxation data. The deformation of methyl geometry from ideal tetrahedrality and corresponding changes in methyl rotational order parameter can also be quantified using NMR experiments.[53] In addition to the above-mentioned examples, various other investigations have used methyl group dynamics as a probe to study protein glass transition,[9,60] protein−ligand binding,[5] hydrophobic core fluidity[61] and crystalline phase transitions.[62] These advances in high-resolution neutron experiments and NMR methods indicate the timeliness of the present study, which can be expected to stimulate corresponding related experimental work.

Acknowledgment. This work was funded by an Oak Ridge National Laboratory Neutron Sciences Laboratory-Directed Research and Development grant from the U.S. Department of Energy.

Supporting Information Available: Complete ref 38. This material is available free of charge via the Internet at http://pubs.acs.org.

JA901276N

(59) Kneller, G. R.; Doster, W.; Settles, M.; Cusack, S.; Smith, J. C. *J. Chem. Phys.* **1992**, *97*, 8864–8879.
(60) Curtis, J. E.; Tarek, M.; Tobias, D. J. *J. Am. Chem. Soc.* **2004**, *126*, 15928–15929.
(61) Best, R. B.; Rutherford, T. J.; Freund, S. M. V.; Clarke, J. *Biochemistry* **2004**, *43*, 1145–1155.
(62) Kavitha, G.; Narayana, C. *J. Phys. Chem. B* **2006**, *110*, 8777–8781.